COBEM 2021 26th International Congress of Mechanical Engineering
ABCM Associação Brasileira de Engenharia e Ciências Mecânicas
November 22-26, 2021, Virtual Congress, Brazil

COB-2021-0349
MANUAL FASTEN TORQUE TOOL DESIGNED AND MANUFACTURED FOR ADDITIVE MANUFACTURING

Luana Seixas Andril Araujo
Luis Fellipe Lopez de Carvalho
Valter Estevão Beal
Luis Antônio Gonçalves Junior
Centro Universitário SENAI CIMATEC, Salvador, BA, Brazil
luandril@gmail.com
fellipelopez78@gmail.com
valter.beal@fieb.org.br
lagjunior@gmail.com

Abstract. *Additive manufacturing (AM) has been used in recent years as a final part manufacturing process. Nevertheless, it maintains its flexibility to produce from one-of-a-kind to recent developments for mass production. In this context, an equipment developed for pre-salt seismic data acquisition needs a hydrophone to capture data. Nevertheless the requirements and constrains of the equipment requires the hydrophone installation on a recessed grove. To install the hydrophone, the assembly team required a special tool for the shape of the hydrophone and it could not scratch the hard anodized aluminum case. The solution was to model a special tool in plastic considering additive manufacturing as the viable alternative. Thus, the torque applied to fasten the hydrophone was carefully calculated. Different tentative designs were made until reach an optimized solution. Two different AM process were considered FDM and MJF and two different materials (PA12 and ABS). The design failure criteria was defined based on the behavior of thermoplastic materials. Topology optimization was employed to avoid material waste. The final design complies with the needs of the assembly team.*

Keywords: *additive manufacturing, thermoplastic failure criteria, topology optimization*

1. INTRODUCTION

With the advancement of industry 4.0, the application of additive manufacturing (AM) has become increasingly frequent, covering several areas, such as medical, aeronautics, automotive, consumer goods, etc. The popularization of these set of technologies is due to its freedom of design and, mainly, to the cost reduction associated with the manufacture of molds, since it allows the obtaining of the final product without the need for the use of additional tooling.

However, products to be manufactured by MA need a specialized development that takes into account the advantages and limitations of the technology, as well as the post-processing of the virtual model. In this context, computational tools have been increasingly used in order to explore all the potential of AM technology. Among them, the topological optimization tools help to obtain the optimized geometric configuration, by removing, for example, the excess mass of the component under development, according to the conditions imposed on it.

From this perspective, there is an equipment developed to collect seismic data from seismic exploration campaigns in the pre-salt. In this equipment, a hydrophone must be present, which is fixed by threading it into the structure. However, access to this hydrophone is difficult due to its location and, for this reason, there was a need to have a tool capable of screwing it into the anodized aluminum structure but without scratching it. The reason for this care is that the equipment shall remain up to five years into the seabed. Any scratch in the anodized surface leads to premature corrosion and possible structural failure. Figure presents a partial section view of the deep recess where the hydrophone is installed. The hydrophone is placed in such manner to avoid mechanical damage during handling of the equipment. The limitation of space to fasten the hexagonal nut at the base of the hydrophone requested the need for a special tool that can accommodate the body of the sensor and tight the nut. Nevertheless, it requires the tool to have lower hardness than the anodized aluminum.

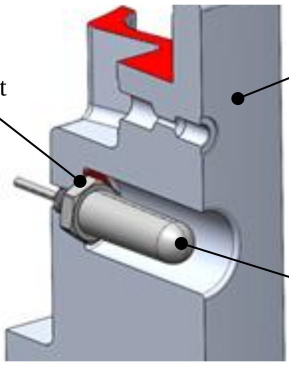

Figure 1. Partial view of the deep recess where the hydrophone is installed in the equipment.

The present work describes the development of a manual torque tool for the fixation of the hydrophone in equipment for the collection of seismic data, taking advantage of the benefits of additive manufacturing, and meeting the necessary criteria to ensure the tightness of the part and the surface integrity of the structure. The approach used brings the conditions adopted to calculate the torque, as well as a study of the polymeric materials used in the final part, and the comparison between them.

2. METHODOLOGY

The tool design was carried out through a research on additive manufacturing, listing the advantages and limitations of this technology. At this stage, a search was also made about the geometric characteristics of the thread used in the hydrophone, in order to obtain the necessary torque for tightening, taking into account the structure material (anodized aluminum), which should not be scratched.

Then, a research related to the polymeric materials adopted for the project was developed, focusing on the selection of those that presented compatible mechanical properties to the level of demands that the component is submitted in operation. Once these properties were obtained, the 3D modeling of three concepts for the tightening tool was performed, using *Solidworks*™ software. Subsequently, the most suitable concept in terms of ergonomics and manufacturing time was selected. Finally, a structural analysis was performed using *Altair Inspire*™ software to assess the strength when subjected to operation loading and a topological optimization simulation to reduce the amount of material used in the component.

The manual torque tool aims to torque the hydrophone on the structure and must be made from a material that resists the imposed demands, in addition to not scratching the anodized aluminum structure of the housing. For this reason, it was decided to make the piece in plastic material.

3.1. Torque Estimation

To perform the calculation of the torque required to secure the hydrophone to the structure, the following premises were adopted:

- The screw has only a fixation function, it is not structural;
- The hydrophone was considered to be entirely made of anodized aluminum to compute the tightening torque. This consideration was made because the hydrophone has a hexagonal part made of titanium, which has a mechanical resistance considerably higher than aluminum alloys;
- 6061 aluminum alloy was adopted for the project due to its good mechanical and corrosion resistance properties. This material has a yield strength of 255 MPa, according to the GGD Metais manufacturer's catalog (GGD, 2021).

To calculate the torque, it was used the Norton (2013) equation (1). Where: T_i is the torque, K_i is the torque coefficient, F_i is the preload value and d is the bolt diameter. According to Shigley, Mischke and Budynas (2005), it is recommended to adopt the value of the torque coefficient as 0.2 when the screw and nut conditions are not declared. The diameter of the screw used in the hydrophone and the type of thread were provided by the manufacturer as 7/16".

$$T_i = K_i F_i d \tag{1}$$

To calculate the preload value, Equation (2) was used, also indicated by Norton (2013), where S_p is the test load and A_t is the screw bolt area. In this case the area is, 77.76 mm^2. Juvinall (2012) defines the proof strength of the screw as the maximum tension that the structure fixed by it supports without causing permanent damage, and its value is slightly lower than the material's yield resistance. With this information, the value of the yield strength of the 6061 aluminum alloy was adopted for S_p.

$$F_i = 0.9 S_p A_t \tag{2}$$

With all this information, the maximum torque value calculated was 35.4 N.m.

3.2 Tool Material Choice

Two materials were analyzed for manufacturing the tool by AM. The first was the ABS-M30 used in the FDM (fused deposition modelling) process. According to the supplier (STRATASYS, 2020), it has a tensile strength of 30 MPa in the XZ printing orientation and 27.5 MPa in the Z orientation (vertical). The thickness of the layer can change according to the machine used therefore it was adopted a layer of 0.254 mm. The other AM material considered was the PA12 for MJF (multi jet fusion). According to HP (2020), the material HR PA 12 GB, has a yield strength range of 28-32 MPa and a density of 1.3 g/cm^3. It is claimed to be a more isotopic material and the construction layer is 0.08 mm.

In possession of the mechanical properties of both materials, a deformation-based failure criterion was defined for the tool under development. According to Erhard (2006), the stress-strain curves of polymers can be described by mathematical models for strains of up to 4%. The mathematical model used can be interpolated by a polynomial of up to 5th degree. From the approximate stress-strain curves of ABS and PA12 (Figure 2 and Figure 3) the 5th order interpolating polynomials were defined to describe the elastic phase behavior of both materials. In the case of ABS, the equation relates to deformation up to 2%; the region where the material starts to flow, and for the PA12 up to a deformation of 4%. Equations 3 and 4 describe the models for the respective materials.

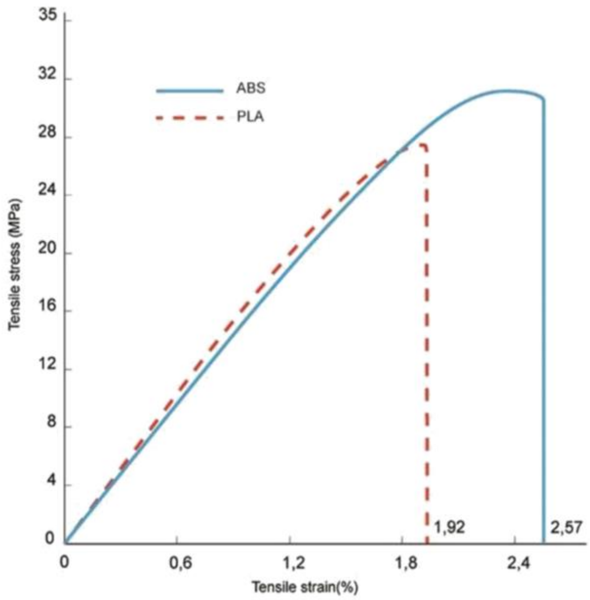

Figure 2. ABS Stress-Deformation Curve (BANJANIN *et al*., 2021).

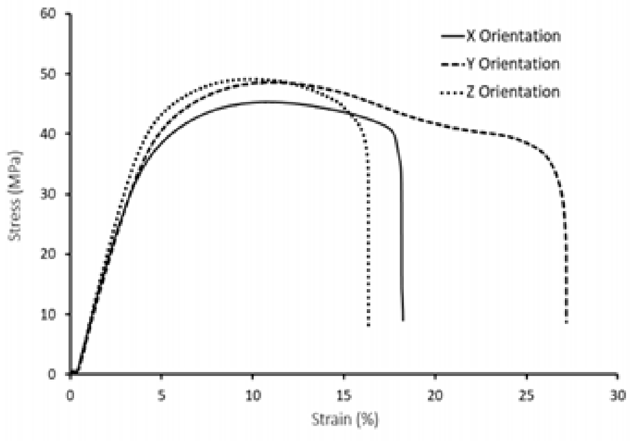

Figure 3. Stress-Deformation Curve of PA12 (O'CONNOR, et al,2018).

$$\boldsymbol{\sigma}(\varepsilon) = -0{,}5095x\varepsilon^5 - 2{,}0601\varepsilon^4 + 2{,}0635\varepsilon^3 - 0{,}3893x\varepsilon^2 + 15{,}281\varepsilon \quad (3)$$

$$\boldsymbol{\sigma}(\varepsilon) = -0{,}0006\varepsilon^5 + 0{,}022\varepsilon^4 - 0{,}2591x\varepsilon^3 + 0{,}4798x\varepsilon^2 + 9{,}5327\varepsilon \quad (4)$$

Erhard (2006), in Figure 3, shows some examples of stress-strain curve behavior of different types of polymers and indicates the best method for each type, as shown in Figure 4. For ABS, one can consider the first example, while for PA12, the third example.

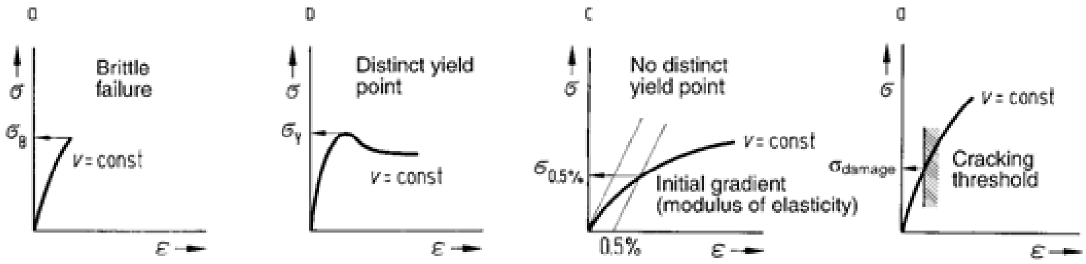

Figure 4. Types of curves that can be used as failure criteria (ERHART, 2006).

As ABS is similar to the first example, where the flow region is well defined, the graph was drawn with the equation found, up to a deformation of 2%. A stress associated with 80% of the flow strain was adopted, because, according to Erhard (2006), this is a good practice when working with polymers. The result can be seen in Figure 5.

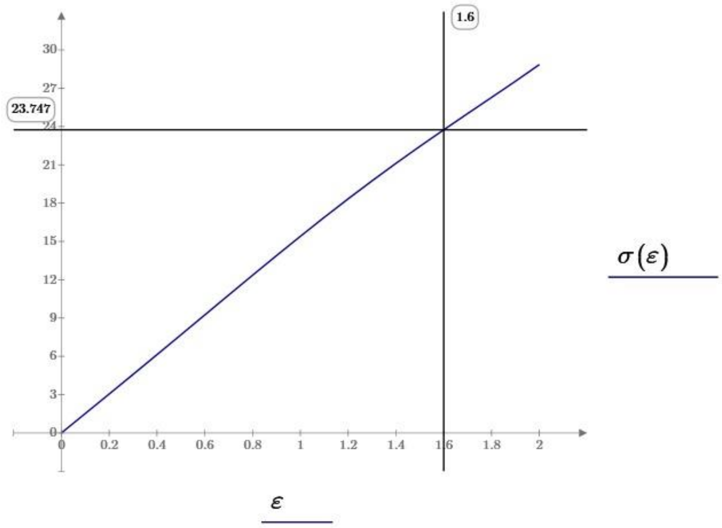

Figure 5. Elastic region of the ABS stress-strain curve interpolated by a 5th order polynomial

The PA12, on the other hand, is similar to the third type of graph present in Figure 3. The graph with the equation found was drawn, for a deformation of up to 4%. Soon after, we found the tangent line of the curve at the origin and displaced it by 0.5%. Then, a new line was drawn from the origin to the point where the 0.5% displaced line intersects the stress-strain curve obtained through the equation. The pair (σ,ϵ) of the intercept defines the yield point of the material. The stress-strain curve interpolated by the 5^{th} degree polynomial is shown in Figure 6.

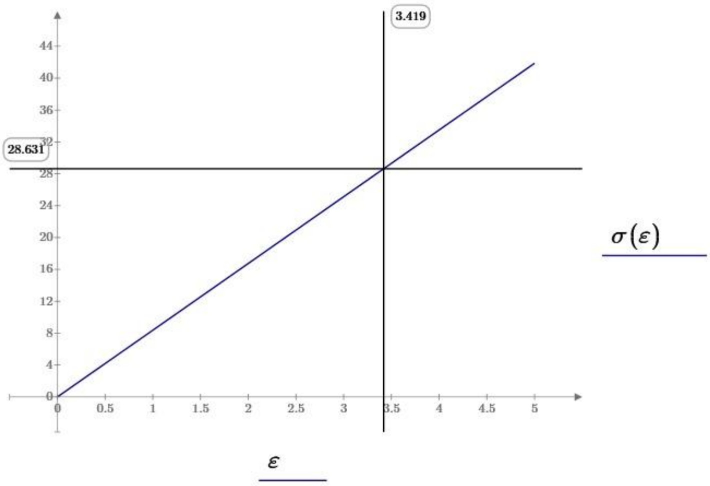

Figure 6. Elastic region of the stress-strain curve of PA12 interpolated by a 5th order polynomial

Therefore, the yield stress that will be adopted for ABS was 23.74 MPa and for PA12, 28.63 MPa.

3.3 Failure Criteria

According to Tavares (2016), most polymers have greater compressive strength than tensile strength, making Von Mises' theory not suitable for these materials. Thus, other criteria that consider these conditions could be used, such as the conically and parabolically modified criteria of von Mises. Nevertheless, In this work, the criteria used was the yield strength. In parallel, von Mises and maximum shear stresses were also evaluated.

3. RESULTS

With the yield stress values found for ABS and PA12, the tightening tool concepts were developed. Altogether, three concepts were developed at this stage. The first concept, as can be seen in Figure 7 (A), showed a good mechanical response to the requests imposed, but does not have restrictions on ergonomics: the region where the operator would hold to generate the torque would end up causing some discomfort and even due to the difficulty of tool in adhering to the user's hand. The second concept had improvements in its handler being more ergonomic than the first concept. It is presented Figure 7 (B). Like concept 1, this one presented a good response to the imposed mechanical efforts, but it had some drawback on other aspects. The separated handle was an attempt to make it cheaper to manufacture. The lower the high, the better the cost for the same amount of material. Additionally, the tool needed an extra operation to assembly.

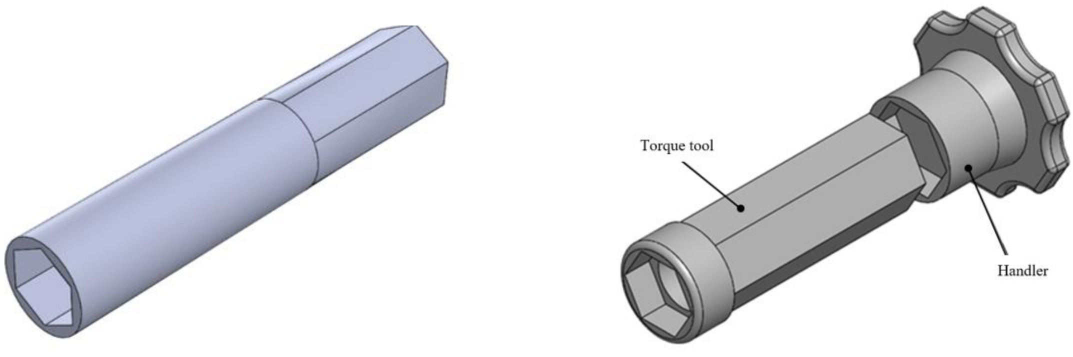

(A) (B)

Figure 7. Fist (A) and second (B) concepts.

The third concept combined the reduction of printing time with good ergonomics. With that, the handle was integrated to the body, as it can be seen in Figure 8. As with the previous concepts, this one also supported the torque well. Figures 9 and 10 show some of the results obtained to evaluate the concept.

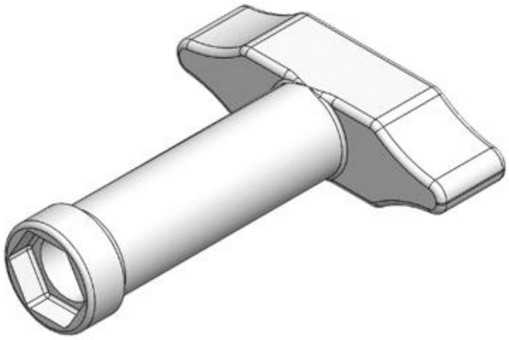

Figure 8. CAD model of the third concept.

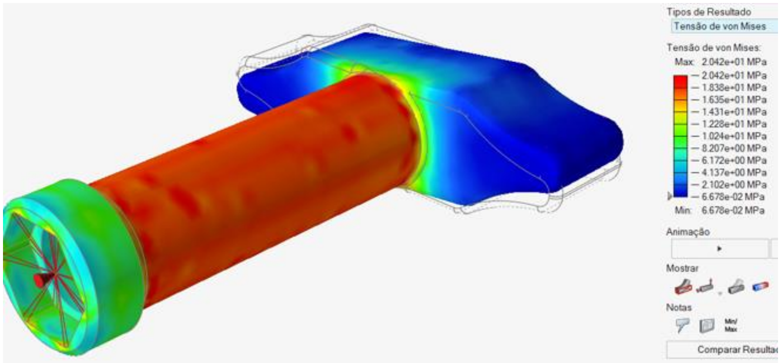

Figure 9. Von Mises plotted results for third concept.

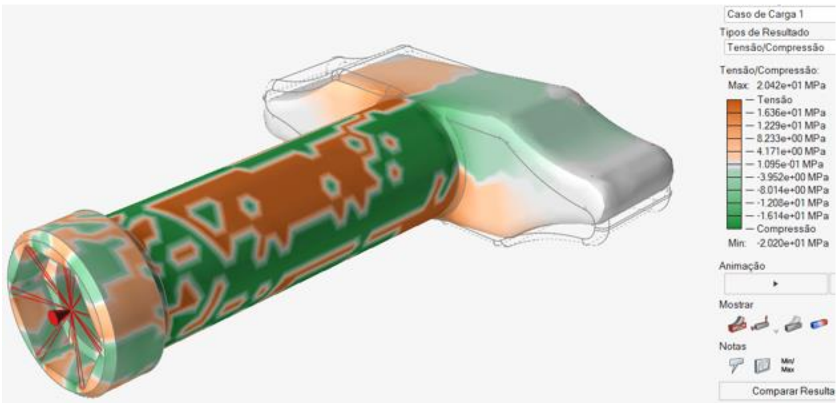

Figure 10. Main compression tensions for the third concept.

Subsequently, a topological optimization simulation was carried out in concept three in order to reduce mass and to make the additive manufacturing faster and cheaper. The final concept developed after performing this optimization simulation is shown in Figure 11.

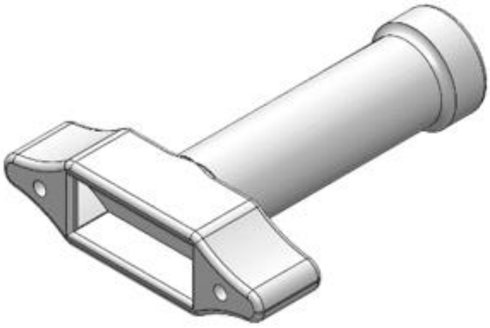

Figure 11. Third concept after topological optimization.

Table 1 shows the comparison between the three concepts, comparing their construction volume and height. Concept two, despite having a smaller volume, has the highest construction height, thus representing a longer printing time.

Table 1. Comparison between the global dimensions of the three concepts developed.

Concept	**Volume (cm^3)**	**Height (mm)**
1	104.,41	35.64
2	59.39	38,00
3	66.13	27.71

The third concept was printed by MJF technology on PA 12 GB on the Additive Manufacturing Bureau at CIMATEC PARK. It is possible see the result in the figure 12. The tool presented toughness and it is ergonomic. The hydrophone adequately fits inside the tool for its installation. Technicians of the seismic node project are using if to assemble the geophones into the prototypes with success.

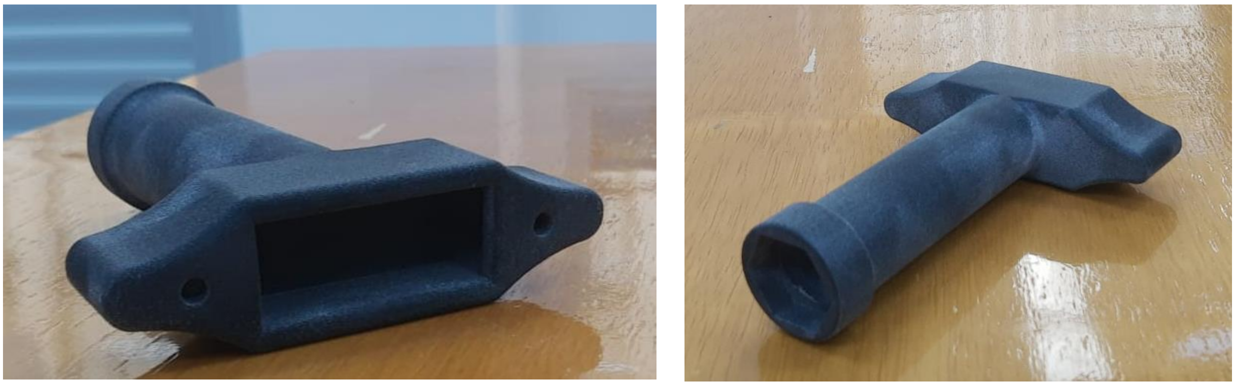

Figure 12. Third concept printed on PA 12 GB using MJF method.

4. CONCLUSIONS

Concept three, despite having a larger volume than concept two, has a lower construction height, which makes the printing process faster and therefore less costly. In addition, another positive aspect is its better ergonomics compared to other models developed. For these reasons, the concept three was chosen as the final concept and it was manufactured and place ready for use.

Due to the complexity of the torque tool geometry, and the need to manufacture few units, additive manufacturing presents itself as a convenient manufacturing process for the manufacture of this component. Using AM FDM method, to produce part with ABS filament represents a cost of U$15.00. For the MJF method using PA 12 GB the costs increases to U$ 38.00. Both material can be used for this design without losing performance. Nevertheless, the MJF shows a near isotropic properties than FDM.

Topology optimization proves to be an excellent tool for helping designers to obtain better and cheaper products with higher performance. Especially when applied in conjunction with additive manufacturing. However, it is important to define the failure criteria to be used for the material. AM materials lacks of information to be used strait forward so designers must be aware of what design failure criteria could be used in every case. Also, the geometry generated by Topology optimization is not always easy to use in the validation analysis. So direct modelling of the geometry based in the topology geometry, like in this case, makes the final validation analysis easier to be performed as the mesh will be more regular to generate.

5. ACKNOWLEDGEMENTS

The authors would like to thank the support of the company HP Brasil Indústria e Comércio de Equipamentos Eletrônicos Ltda, SENAI CIMATEC and SHELL do Brasil. This project was funded by HP Brasil using resources based on Law #8.248 of 1982 (Lei da Informática).

6. REFERENCES

Banjamin, Bojan; Vladic, Gojko; Pál, Magdolna; Balos, Sebastian; Dramicanin, Miroslav; Rochov, Milan; Knezevic, Ivan. “Consistency analysis of mechanical properties of elements produced by FDM additive manufacturing technology”. https://www.scielo.br/scielo.php?script=sci_arttext&pid=S1517-70762018000400441. Accessed: 18 february 2021.

Erhard, Gunter. “Designing with plastics”. Munich. Hanser Publications. 2006.

GGD Metais. “Alumínio”, https://www.ggdmetals.com.br/wp-content/uploads/2015/07/aluminio.pdf; Material Data Sheet.2015

HP. “HP 3D Printing materials for the HP Jet Fusion 5200 Series 3D Printing Solution Mechanical Properties” White Paper. https://www.hp.com/us-en/printers/3d-printers/materials.html. September 2020.

Juvinall, Robert C.; Marshek, Kurt M. “Fundamentals of Machine Component Design” 5th Ed. New Jersey: John Wiley & Sons, Inc., 2012.

Norton, Robert L. “Projeto de Máquinas: uma abordagem integrada”, 4th Ed. Porto Alegre, Bookman, 2013.

O’Connor, Heather J.; Dickson, Andrew N.; Dowling, Denis P. “Evaluation of the mechanical performance of polymer parts fabricated using a production scale multi jet fusion printing process”, School of Mechanical and Materials Engineering, University College Dublin, Ireland. 2018.

Shigley, Joseph E.; Mischke, Charles R.; Budynas, Richard G. “Projeto de Engenharia Mecânica” 7. ed. Porto Alegre: : Bookman, 2005.

Stratasys, “ABS-M30 – FDM Thermoplastic Filament”, https://www.stratasys.com/materials/search/abs-m30; Material Data Sheet. 2020.

Tavares, Daniel Barduzzi**. “**Desenvolvimento e validação numérico-experimental de corpo de prova unificado para ensaios mecânicos de polímeros termoplásticos injetados**”.** 2016. 152 f. Dissertação (Mestrado) - Curso de Engenharia Mecânica, Centro Universitário Fei, São Bernardo do Campo, 2016. Disponível em: http://sofia.fei.edu.br:8080/pergamumweb/vinculos/000033/000033e5.pdf. Accessed: 17 march. 2021.

7. RESPONSIBILITY NOTICE

The authors are the only responsible for the printed material included in this paper.